Genome-wide transcriptional analysis of differentially expressed genes in flagellin-pretreated mouse corneal epithelial cells in response to *Pseudomonas aeruginosa:* involvement of S100A8/A9

N Gao[1], G Sang Yoon[2], X Liu[2,3], X Mi[1], W Chen[4], TJ Standiford[5] and F-SX Yu[1,2]

We previously showed that pre-exposure of the cornea to Toll-like receptor 5 ligand flagellin induces profound mucosal innate protection against infections by modifying gene expression. Taking advantage of easily procurable epithelial cell population, this study is the first report to use genome-wide cDNA microarray approach to document genes associated with flagellin-induced protection against *Pseudomonas aeruginosa* in corneal epithelial cells (CECs). Infection altered the expression of 675 genes (497 up and 178 down), while flagellin pretreatment followed by infection resulted in a great increase in 890 gene upregulated and 37 genes downregulated. Comparing these two groups showed 209 differentially expressed genes (157 up, 52 down). Notably, among 114 genes categorized as defense related, S100A8/A9 are the two most highly induced genes by flagellin, and their expression in the corneal was confirmed by realtime PCR and immunohistochemistry. Neutralization of S100A8 and, to a less extent, A9, resulted in significantly increased bacterial burden and severe keratitis. Collectively, our study identifies many differentially expressed genes by flagellin in CECs in response to *Pseudomonas*. These novel gene expression signatures provide new insights and clues into the nature of protective mechanisms established by flagellin and new therapeutic targets for reducing inflammation and for controlling microbial infection.

INTRODUCTION

The protective ability of innate defense is largely dependent on germ-line-encoded pattern-recognition receptors.[1] Prominent among pattern-recognition receptors are the Toll-like receptors (TLRs) that recognize pathogen-associated molecular patterns to initiate innate immune responses, including inflammatory mediators, antimicrobial effectors, and signals inducing adaptive immune responses.[2] Discovery of TLRs and other pathogen-associated molecular pattern-recognizing receptors has also put the epithelium, a barrier between internal and external environments, at center stage not only in defending the host against infection at the front line but also in influencing the development and direction of immune cell response to ensure clearance of the invading pathogen.[3–8] A large body of recent literature revealed that mucosal epithelia, including the ocular surface, express almost all TLRs, rendering them able to sense and to mount the innate defense against invading pathogens.[9] Conversely, the epithelial innate and inflammatory response to pathogens, if not properly controlled, can also cause tissue damage, resulting in the development of human diseases, such as corneal haze and scarring,[10] airway asthma,[11] and allergic rhinitis.[12] Multiple regulatory mechanisms exist in epithelial

[1]Department of Ophthalmology, Wayne State University School of Medicine, Detroit, Michigan, USA. [2]Department of Anatomy and Cell Biology, Wayne State University School of Medicine, 4717 St, Antoine Street, Detroit, Michigan, USA. [3]Department of Ophthalmology, Peking Union Medical College Hospital, Chinese Academy of Medical Sciences, Beijing, China. [4]Genomic Core Lab of National Institute of Diabetes and Digestive and Kidney Diseases, Bethesda, Maryland, USA and [5]Division of Pulmonary and Critical Care Medicine, Department of Internal Medicine, University of Michigan Medical Center, Ann Arbor, Michigan, USA. Correspondence: F-SX Yu (fyu@med.wayne.edu)

Received 16 October 2012; accepted 10 December 2012; published online 23 January 2013. doi:10.1038/mi.2012.137

cells to control the inflammatory response, including the expression of negative regulators[13] and induction of hyporesponsiveness, to further and more rigorously challenge the same or different pathogens, a phenomenon similar to endotoxin tolerance.[14] It is now well-known that pre-exposure of different cells, tissues, or organisms to TLR ligands dampens the expression of inflammatory cytokines, while exhibits no effect or even augments the induced expression of other functional groups of genes such as antimicrobial, anti-oxidative, and/or cytoprotective genes in response to pathogens and other adverse challenges, a phenomenon similar to endotoxin tolerance or lipopolysaccharide-reprogramed TLR response.[15–18]

As an immune-privileged site, the avascular cornea contains mechanisms that limit immune cell entry and has scant antigen-presenting cells.[19,20] Under normal conditions, the cornea is remarkably resistant to infection. However, when the epithelial barrier is breached, which often occurs during routine contact lens wearing, or when immune function is compromised, opportunistic pathogens can gain access to the deep layers of the epithelium, causing infectious keratitis.[21–24] If not treated promptly and properly, significant vision loss or even loss of the eye may occur.[25–27] Among pathogens, *Pseudomonas aeruginosa* is a major cause of keratitis and is the most sight threatening.[28] Our previous work showed that *P. aeruginosa* is recognized by TLR5 and that mice deficient in TLR5 are more susceptible to the pathogens.[18,22,29] We have also shown that application of purified flagellin, the ligand of TLR5, before microbial inoculation induces profound protection in the cornea against infectious pathogens regardless of whether or not they express flagellin.[17,18] Similar protection against *P. aeruginosa* was also observed in the lung by nasal application of flagellin.[30] In addition, flagellin was also reported to induce protection against lethal radiation and chemicals in mice and monkeys,[31,32] to restore antibiotic-impaired innate immune defenses,[33] and to protect mice from acute *Clostridium difficile* colitis.[34] Among all known TLR ligands, the flagellin–TLR5 axis, but not the flagellin–Ipaf pathway,[35,36] exhibits several distinctive properties: stimulating mucosal epithelial cells more than immune cells,[37] inducing unique anti-inflammatory genes (such as interleukin (IL)-1Ra, but not IL-1β),[32,38] and preserving epithelial barrier function.[33,34] However, to date, a genome-wide screen for genes and pathways affected by flagellin preconditioning in the mucosal epithelia and their roles in subsequent protection of mucosal tissues have not been reported.

In this study, we took advantage of the topical application of flagellin and readily isolated epithelial cells from the cornea and used genome-wide cDNA microarray to profile gene expression in *P. aeruginosa*–infected CECs with or without flagellin pretreatment. We identified 1261 genes with more than two fold changes ($n = 6$, $P < 0.05$) in response to infection; among those, 209 genes were altered by flagellin pretreatment. Targeting the 2 most highly induced genes, S100A8 and S100A9, we found that neutralizing these two proteins increased susceptibility of the cornea to *P. aeruginosa* infection and abolished flagellin-induced protection in B6 mice. Based on data mining, we constructed a corneal innate defense network, activation of which promotes mucosal innate immunity and renders tissue resistance to invading pathogens.

RESULTS

Flagellin-induced protection

We previously showed that flagellin preconditioning resulted in the resistance to ocular and lung pathogenic microbes with or without expressing flagellin, suggesting a general, broad innate protection against infection. We reasoned that genes differentially expressed in flagellin-pretreated and *P. aeruginosa*–infected corneas, compared with *P. aeruginosa*–infected corneas, are responsible for the innate protection observed in the cornea and performed genome-wide microarray expression analysis to compare genes expressed in *P. aeruginosa*–infected corneal epithelial cells (CECs) with or without flagellin pretreatment at 6 hours post-infection (hpi; **Figure 1**). In our previous studies, we used *P. aeruginosa* ATCC 19660 strain, the most virulent strain, to illustrate the profound mucosal protective effects. However, as ATCC 19660 is known to possess epithelial cytotoxicity and cause epithelial erosion, we used a laboratory strain PA01 with 10-fold in inoculate dosage, 10^5 colony-forming units (CFU)/per eye in phosphate-buffered saline (PBS). As our focus was on differentially expressed genes in flagellin-pretreated CECs, we prepared three biological replicates of CECs obtained directly by scrapping cells off from the corneas: scratched and topical applied 5 μl PBS or 500 ng purified flagellin in 5 μl PBS, followed by 1×10^5 PA01 infection, with no injury and no infection naive CECs as the control. The six-sample (array spot) Illumina MouseWG-6 v2 BeadChip (San Diego, CA) was used. Each array spot contains a total of 45,281 different oligonucleotide gene probes (i.e., Illumina source IDs,). After the normalization of raw data for all three replicates, we selected those genes that exceeded a pre-set threshold for significant changes $\geq$2-fold (both increase or decrease) in expression intensity between infected/normal, pretreated-infected/normal, and pretreated-infected/infected. Of the genes present on the array, 1,261 were found to have altered expression at least in one of three paired comparisons with $P < 0.05$ (**Supplementary Information**). As shown in **Figure 1**, there were a total of 675 genes, compared with the control, with altered expression in PA01-infected CECs at 6 hpi, 497 up- and 178 downregulated. In flagellin-pretreated CECs, 890 genes were upregulated but only 39 were downregulated. Comparing PA01-infected CECs with or without flagellin pretreatment revealed a total of 209 genes with altered expression; 157 up- and 52 down regulated.

The top six genes upregulated in CECs in response to PA01 infection are matrix metallopeptidase 13 (Mmp13; 80.2-fold increase), S100A8 (36.3), Mmp10 (34.2), Krt16 (32.7), Stfna1l1 (31.2), and S100A8-binding partner S100A9 (27.5) (**Table 1**). Expression of these genes in flagellin-pretreated and infected CECs, compared with infected CECs, were either downregulated: MMP13 5.4-fold, MMP10 4.1-fold and

Stfna1l1 2.3-fold decrease; no significant change for Krt16; or upregulated: S100A8 4.2-fold and S100A9 2.54-fold increase, bringing the total increase of these two genes over the control to 154- and 69.8-fold, respectively. These changes reflected the functions of the genes and their contribution to flagellin-induced protection, including greatly increasing bacterial clearance (S100A8/A9 also named calprotectin, a potent antimicrobial protein complex[39–41]), and suppression of potential harmful genes (MMP13 and -10). Interestingly, stefin A1-like 1 (an intracellular cycteine-type endopeptidase inhibitor) was also downregulated 2.3-fold. Stfna1l1 was implicated as a component of proteasomes, and its substrate and function were not reported in the literature. Taken together, the genome-wide cDNA microarray revealed that flagellin preconditioning favors the expression of a large number of mucosal innate protective genes while controlling but not totally blocking genes that are part of innate response to infection and yet can be destructive when their activities are not well-controlled.

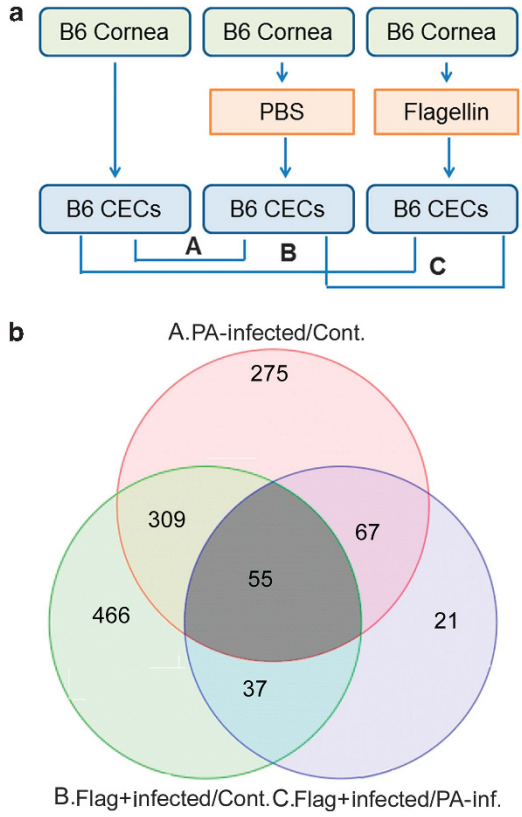

Figure 1 Expression profiling of genes regulated by PA01 with or without flagellin pretreatment. (**a**) B6 mouse corneas were needle scratched and instilled topically with 500 ng flagellin in 5 μl or 5 μl phosphate-buffered saline (PBS) as for 24 h and then re-scratched and inoculated with 1.0×10^5 CFU (colony-forming units) of PA01. At 6 hpi (hours post infection), epithelial cells scraped off from the corneas were harvested for expression profiling, with epithelial cells from naive mouse corneas as the control (Cont.). Binary comparisons were made as indicated, creating differential expression profiles and significance measures corresponding to the indicated effects, each based on the mean and variance of three independent experiments. (**b**) Venn diagrams indicating overlap of genes induced due to infection, flagellin pretreatment/infection. Numbers of overlapped and non-overlapped genes are in different shaded areas. The cutoff values are twofold difference with the *P* values < 0.05. CEC, corneal epithelial cell; PA, *Pseudomonas aeruginosa*.

Flagellin-induced defense response in PA01-infected cornea epithelia

Gene ontology analyses carried out by the Genomatrix Genome Analyzer (Ann Arbor, MI) revealed that 113 genes participate in cell defense response and its regulation, starting from transcription factors in the nuclei to secreted proteins/peptides in extracellular milieu. The full names of the genes, their expression levels, and their cellular localizations are listed in **Table 2**. Chi3l1 has recently been shown to promote *Streptococcus pneumoniae* killing and to augment host tolerance to lung antibacterial responses,[42] we therefore added it to the list as a defense-responsive gene to **Table 2** and **Figure 7**. There were a total 30 nuclear proteins, many of which are the components of a transcription factor family, such as NFKBIZ, NFKB1 (precursor of p50), and NFKBIA for nuclear factor (NF)-κB, and JUN and FOS for AP-1. As expected, NF-κB components were generally downregulated by flagellin pretreatment, resulting in hyporesponsiveness of cells to bacterial challenge in terms of production of NF-κB-mediated pro-inflammatory cytokines, such as C-X-C motif chemokine ligand 1 (CXCL1) and IL-1β. On the other hand, four interferon (IFN) regulatory factors (IRFs) either remained elevated (IRF1 and 6) or further augmented (IRF 7 and 9) in flagellin-pretreated CECs. There were 33 cytosolic proteins, some of which are involved in antiviral and innate responses (ISG15, S100A14, and LTF). Twenty membrane proteins were identified, including IFN receptors and IFN-induced membrane proteins with antimicrobial activities (IFNGR1, IFNGR2, IFITM1, and IFITM2), consistent with elevated expression of multiple IRFs. Most importantly, there were a

Table 1 Top six highly PA01-induced genes and their regulation by flagellin pretreatment

SYMBOL	Gene title	*P*-value	Inf. vs. C	*P*-value	Flag-inf vs. C	*P*-value	Flag-inf. vs. inf.
Mmp13	Matrix metallopeptidase 13	2.74E-11	80.1652	7.54E-09	14.8848	1.36E-06	−5.3857
S100a8	S100 calcium-binding protein A8	2.21E-08	36.3138	6.11E-10	154.02	0.00015	4.24136
Mmp10	Matrix metallopeptidase 10	7.26E-08	34.198	1.47E-05	8.42531	0.00062	−4.05896
Krt16	Keratin 16	3.82E-06	32.6831	2.44E-06	38.1349	0.7299	1.16681
Stfna1l1	Stefins A1-like 1	8.89E-07	31.2961	1.37E-05	13.3889	0.03398	−2.33747
S100a9	S100 calcium-binding protein A9	4.13E-10	27.4806	2.84E-11	69.8298	0.00013	2.54105

Table 2 PA01-induced and flagellin-mediated defense response genes

		Infected vs. normal		Flag-infected vs. normal		Flag-infected vs. infected		
Gene symbol	Description	*P*-value	Fold-change	*P*-value	Fold-change	*P*-value	Fold-change	Cellular location
IRF7[a]	Interferon regulatory factor 7	0.51536	1.10901	3.91E-07	5.15553	7.53E-07	4.64876	Nucleus
SP100[a]	SP100 nuclear antigen	0.158511	1.22956	2.13E-05	2.61884	0.000177	2.12989	Nucleus
IRF9[a]	Interferon regulatory factor 9	0.000145	2.36209	4.47E-07	4.92542	0.000514	2.0852	Nucleus
TRAFD1	TRAF-type zinc finger domain containing 1	0.069651	1.31223	1.78E-05	2.64229	0.000306	2.01358	Nucleus
HIST1H2BC	Histone cluster 1, H2bc	0.422054	1.29191	0.01606	2.39276	0.069981	1.85212	Nucleus
STAT1[a]	Signal transducer and activator of transcription 1, 91kDa	0.138359	1.29412	0.000248	2.35606	0.00342	1.82059	Nucleus/cyto.
PML[a]	Promyelocytic leukemia	0.047309	1.31408	2.20E-05	2.36104	0.000563	1.79672	Nucleus
SAMHD1	SAM domain and HD domain 1	0.001422	2.05283	2.22E-05	3.30108	0.017554	1.60806	Nucleus
ELF3[a]	E74-like factor 3 (ets domain TF, epithelial-specific)	0.073859	1.59088	0.003721	2.36666	0.119162	1.48764	Nucleus/cyto.
SMAD1[a]	SMAD family member 1	0.037533	1.53357	0.00179	2.09529	0.112362	1.36628	Nucleus
PCBP2	Poly(rC)-binding protein 2	0.152515	1.5209	0.02637	2.01211	0.326908	1.32298	Nucleus/cyto.
IRF1[a]	Interferon regulatory factor 1	0.049151	1.60282	0.005609	2.07975	0.247729	1.29756	Nucleus
HSP90AB1	Heat shock protein 90kDaα, class B member 1	0.030182	2.27782	0.007928	2.91858	0.469609	1.2813	Multiple
JAK1	Janus kinase 1	0.019179	1.7061	0.003512	2.05573	0.359276	1.20493	Nucleus
NFKBIZ	Nuclear factor of kappa light polypeptide gene enhancer in B-cells inhibitor, zeta	0.000122	2.67351	0.00013	2.65498	0.969244	−1.00698	Nucleus/cyto.
CEBPG[a]	CCAAT/enhancer-binding protein (C/EBP), gamma	0.000187	2.22473	0.000209	2.20027	0.940763	−1.01112	Nucleus
IRF6[a]	Interferon regulatory factor 6	0.010491	2.21454	0.011646	2.18134	0.954401	−1.01522	Nucleus
HSPD1	Heat shock 60kDa protein 1 (chaperonin)	0.009322	2.41196	0.016274	2.21037	0.761036	−1.0912	Multipe
FOS[a]	FBJ murine osteosarcoma viral oncogene homolog	0.009169	2.03559	0.04916	1.65126	0.379238	−1.23275	Nucleus
IRGM	Immunity-related GTPase family, M	4.83E-06	4.26351	2.57E-05	3.40225	0.247826	−1.25314	Nucleus
JUN[a]	Jun proto-oncogene	4.08E-06	2.21395	0.000184	1.70284	0.022346	−1.30015	Nucleus
NFKB1	Nuclear factor of kappa light polypeptide gene enhancer in B-cells 1	1.35E-06	2.71911	0.000176	1.83146	0.004477	−1.48467	Nucleus/cyto.
NFKB1[a]	NF of κ light polypeptide gene enhancer in B-cells 1	1.35E-06	2.71911	0.000176	1.83146	0.004477	−1.48467	Nucleus/cyto.
JAK2	Janus kinase 2	1.10E-05	2.59087	0.001344	1.73262	0.010299	−1.49535	Nucleus
Jak2	Janus kinase 2	1.10E-05	2.59087	0.001344	1.73262	0.010299	−1.49535	Nucleus
HIF1A[a]	Hypoxia inducible factor 1, alpha subunit	0.000271	2.86239	0.008489	1.89686	0.064399	−1.50902	Nucleus
CEBPB[a]	CCAAT/enhancer-binding protein (C/EBP), β	5.69E-05	3.87288	0.002836	2.26818	0.029694	−1.70748	Nucleus/cyto.
TNFAIP3	TNFα-induced protein 3	5.63E-08	5.68342	1.32E-05	2.81836	0.00045	−2.01657	Nucleus
BCL3[a]	B-cell CLL/lymphoma 3	3.32E-10	6.70447	1.32E-07	3.0733	6.24E-06	−2.18152	Nucleus
NFKBIA	IkappaBalpha	0.000547	3.48829	0.132261	1.52584	0.008736	−2.28615	Nucleus/cyto.
EGR1[a]	Early growth response 1	0.795012	1.15499	0.090924	−2.72613	0.05768	−3.14866	Nucleus
ISG15	ISG15 ubiquitin-like modifier	0.061282	1.74262	6.76E-07	14.7154	6.49E-06	8.4444	Cytoplasm
OAS2	2'-5'-oligoadenylate synthetase 2, 69/71kDa	0.004938	1.79889	2.75E-08	10.0861	5.57E-07	5.60685	Cytoplasm
XAF1	XIAP associated factor 1	0.000532	2.1492	6.26E-08	7.54388	7.20E-06	3.51009	Cytoplasm
IFITM3	Interferon-induced transmembrane protein 3	1.58E-07	4.87348	4.13E-10	16.195	2.51E-06	3.32309	Cytoplasm
DHX58	DEXH (Asp-Glu-X-His) box polypeptide 58	0.024163	1.39272	1.58E-07	4.38151	2.01E-06	3.14602	Cytoplasm
USP18	Ubiquitin specific peptidase 18	1.08E-05	5.25499	1.12E-07	13.9647	0.000953	2.65742	Cytoplasm
LTF	Lactotransferrin	0.588422	1.19456	0.005413	3.00677	0.014596	2.51706	Cytoplasm
GCH1	GTP cyclohydrolase 1	5.56E-06	2.6455	2.53E-08	5.27164	0.000125	1.99268	Cytoplasm
APOBEC1	Apolipoprotein B mRNA editing enzyme, catalytic polypeptide 1	0.546388	1.13101	0.002325	2.1787	0.006901	1.92633	Cytoplasm
RSAD2	Radical S-adenosyl methionine domain containing 2	0.000303	4.62087	2.16E-05	7.76524	0.114925	1.68047	Cytoplasm
PSMB8	Proteasome subunit, beta type, 8	0.169438	1.73613	0.016292	2.89413	0.200373	1.667	Cytoplasm
DDX58	DEAD (Asp-Glu-Ala-Asp) box polypeptide 58	0.050962	1.46438	0.000372	2.40996	0.015505	1.64572	Cytoplasm
MAP2K1	Mitogen-activated protein kinase kinase 1	0.021927	1.77802	0.00049	2.86454	0.04924	1.61108	Cytoplasm
MX2	Myxovirus (influenza virus) resistance 2 (mouse)	0.049503	1.40197	0.000263	2.24186	0.01074	1.59907	Cytoplasm
S100A14	S100 calcium-binding protein A14	0.021966	3.17889	0.003959	4.82976	0.355747	1.51932	Cytoplasm
EIF2AK2	Eukaryotic translation initiation factor 2-alpha kinase 2	0.000226	1.95477	4.16E-06	2.84746	0.011772	1.45668	Cytoplasm

Table 2 (Continued)

Gene symbol	Description	Infected vs. normal		Flag-infected vs. normal		Flag-infected vs. infected		Cellular location
		P-value	Fold-change	*P*-value	Fold-change	*P*-value	Fold-change	
ADAR	Adenosine deaminase, RNA-specific	0.005782	1.55938	5.83E-05	2.27053	0.014778	1.45604	Cytoplasm
YWHAZ	Tyrosine 3-monooxygenase/tryptophan 5-monooxygenase activation protein, zeta polypeptide	0.069065	1.46427	0.002825	2.06232	0.097818	1.40843	Cytoplasm
PRDX5	Peroxiredoxin 5	0.109073	1.47637	0.007606	2.07156	0.15774	1.40314	Cytoplasm
CDO1	Cysteine dioxygenase, type I	3.43E-05	−2.33236	0.001197	−1.72982	0.037774	1.34833	Cytoplasm
HSP90AB1	Heat shock protein 90kDaα (cytosolic), class B member 1	0.030182	2.27782	0.007928	2.91858	0.469609	1.2813	Cytoplasm
ube2n	Ubiquitin-conjugating enzyme E2N	0.040128	1.72389	0.008112	2.12665	0.388974	1.23363	Cytoplasm
PTPN1	Protein tyrosine phosphatase, non-receptor type 1	0.012095	1.99887	0.003519	2.34843	0.499698	1.17488	Cytoplasm
NLRX1	NLR family member X1	0.005433	1.94667	0.0025	2.12138	0.664894	1.08975	Cytoplasm
GSTP1	Glutathione S-transferase pi 1	0.026808	1.89181	0.014856	2.05445	0.74731	1.08597	Cytoplasm
SOCS6	Suppressor of cytokine signaling 6	0.000406	2.09302	0.000358	2.1177	0.938227	1.01179	Cytoplasm
MYD88	Myeloid differentiation primary response gene (88)	0.000225	2.27221	0.000475	2.11167	0.640665	−1.07603	Cytoplasm
HSPD1	Heat shock 60kDa protein 1 (chaperonin)	0.009322	2.41196	0.016274	2.21037	0.761036	−1.0912	Cytoplasm
BCL10	B-cell CLL/lymphoma 10	3.00E-06	2.28395	1.90E-05	1.98742	0.193723	−1.1492	Cytoplasm
DUSP7	Dual specificity phosphatase 7	3.44E-06	3.69737	0.000135	2.44088	0.024882	−1.51477	Cytoplasm
SBNO2	Strawberry notch homolog 2 (Drosophila)	8.10E-06	2.62494	0.0022	1.65622	0.004081	−1.5849	Cytoplasm
Sbno2	Strawberry notch homolog 2 (Drosophila)	8.10E-06	2.62494	0.0022	1.65622	0.004081	−1.5849	Cytoplasm
SOCS3	Suppressor of cytokine signaling 3	0.000319	8.99332	0.048015	2.58296	0.013837	−3.48179	Cytoplasm
IFI27	Interferon, alpha-inducible protein 27	0.436113	1.25338	9.38E-07	15.3115	2.20E-06	12.2162	M Membrane
BST2	Bone marrow stromal cell antigen 2	0.281809	1.22368	3.13E-06	4.66776	1.19E-05	3.81452	Golgi apparatus
IFITM1	Interferon-induced transmembrane protein 1	0.077827	1.52453	2.82E-05	4.40229	0.000479	2.88764	Cell Membrane
IFITM2	Interferon-induced transmembrane protein 2	0.00601	1.68559	1.68E-06	4.12321	0.000117	2.44616	Cell Membrane
GBP2	Guanylate-binding protein 2, IFN-inducible	0.079648	1.52856	0.000102	3.66391	0.002165	2.39697	Cell Membrane
CD8B	CD8b molecule	8.17E-05	−2.02671	0.220707	−1.16967	0.000688	1.73272	P Membrane
F2R	Coagulation factor II (thrombin) receptor	8.18E-06	−2.6071	0.003663	−1.5925	0.002479	1.63712	P Membrane
OSMR	Oncostatin M receptor	0.000903	1.9475	4.27E-05	2.63016	0.067472	1.35053	M membrane
BCL2	B-cell CLL/lymphoma 2	0.00031	−2.03885	0.006683	−1.594	0.109761	1.27908	M membrane
IFNGR2	Interferon gamma receptor 2	0.02024	1.90289	0.007121	2.18633	0.570234	1.14896	Membrane
FAIM3	Fas apoptotic inhibitory molecule 3	0.000325	1.94655	0.000101	2.15268	0.453915	1.1059	Membrane
ANXA1	Annexin A1	1.13E-05	4.84605	9.21E-06	5.01949	0.869516	1.03579	P Membrane
TFRC	Transferrin receptor (p90, CD71)	4.37E-05	3.24094	0.000103	2.90335	0.55496	−1.11627	P Membrane
IFNGR1	Interferon gamma receptor 1	1.10E-06	3.69699	6.30E-06	3.01819	0.187901	−1.2249	P Membrane
TNFRSF1A	TNF receptor superfamily, member 1A	0.000808	2.13404	0.016552	1.59796	0.109212	−1.33547	P Membrane
LTB4R	Leukotriene B4 receptor	1.22E-05	3.13629	0.000302	2.23702	0.057132	−1.40199	P Membrane
ADORA2B	Adenosine A2b receptor	7.11E-05	2.76577	0.002171	1.92857	0.051597	−1.43411	P Membrane
CD44	CD44 molecule (Indian blood group)	1.32E-05	4.62088	0.000152	3.19812	0.101889	−1.44487	P Membrane
ITGB6	Integrin, beta 6	6.34E-09	5.04524	1.29E-05	2.21894	9.56E-06	−2.27372	P Membrane
ICAM1	Intercellular adhesion molecule 1	5.28E-09	6.78982	1.34E-05	2.521	6.74E-06	−2.6933	P Membrane
LGALS3BP	Lectin, galactoside-binding, soluble, 3 binding protein	0.114266	1.39806	6.79E-08	11.8169	3.03E-07	8.45235	Secreted
IFIT3	IFN-induced protein with tetratricopeptide repeats 3	0.043905	2.63634	5.42E-05	14.9829	0.001826	5.68322	Cyto/secreted
B2M	β-2-microglobulin	0.003516	2.13397	1.16E-07	11.7143	4.56E-06	5.48946	Secreted
S100A8	S100 calcium-binding protein A8	2.21E-08	36.3138	6.11E-10	154.02	0.000145	4.24136	Cyto/secreted
Chi3l1	Chitinase 3-like 1 (cartilage glycoprotein-39)	0.001137	4.40342	6.64E-06	15.1109	0.003982	3.43164	Secreted
CXCL10	Chemokine (C-X-C motif) ligand 10	0.708221	1.08622	6.23E-05	3.64897	0.000113	3.35934	Secreted
LCN2	Lipocalin 2	0.029482	2.3174	0.000117	7.05984	0.006901	3.04644	Secreted
S100A9	S100 calcium-binding protein A9	4.13E-10	27.4806	2.84E-11	69.8298	0.000125	2.54105	cyto/secreted
CFB	Complement factor B	0.766377	1.04103	1.63E-05	2.60608	2.42E-05	2.50337	Secreted
IL15	Interleukin 15	0.877282	−1.02468	0.00014	2.4058	0.000111	2.46517	Secreted
PGLYRP4	Peptidoglycan recognition protein 4	0.027166	1.55242	8.69E-06	3.625	0.000399	2.33507	Secreted
Apol7a	Apolipoprotein L, 3 (human)	0.795086	−1.05631	0.003141	2.16983	0.001987	2.29202	Secreted

Table 2 (Continued)

Gene symbol	Description	Infected vs. normal		Flag-infected vs. normal		Flag-infected vs. infected		Cellular location
		P-value	Fold-change	*P*-value	Fold-change	*P*-value	Fold-change	
PGLYRP1	Peptidoglycan recognition protein 1	0.164294	−1.14491	1.14E-05	1.92439	1.68E-06	2.20325	Secreted
IFI35	Interferon-induced protein 35	0.134494	1.30361	9.04E-05	2.67338	0.001106	2.05075	Cyto/secreted
C3	Complement component 3	0.039871	1.4769	3.91E-05	3.01314	0.001342	2.04017	Secreted
LY96	Lymphocyte antigen 96	0.033754	1.46302	0.000174	2.38787	0.009729	1.63216	Secreted
DEFB1	Defensin, beta 1	0.015749	2.00685	0.000803	3.05398	0.1136	1.52178	Secreted
CST3	cystatin C	0.118388	1.38634	0.003283	2.05592	0.065736	1.48298	Secreted
PPBP	Pro-platelet basic protein (chemokine (C-X-C motif) ligand 7)	0.026004	2.55941	0.021646	2.65552	0.922327	1.03755	Secreted
IL1RN	Interleukin 1 receptor antagonist	5.06E-08	2.64206	2.52E-07	2.31599	0.131153	−1.14079	Secreted
TNF	Tumor necrosis factor	1.08E-05	2.49795	9.49E-05	2.06984	0.1646	−1.20683	Cyto/secreted
IL1A	Interleukin 1, alpha	4.71E-05	3.26766	0.000382	2.51774	0.182952	−1.29786	Secreted
CCL4	Chemokine (C-C motif) ligand 4	0.012826	2.01984	0.305991	1.29354	0.088875	−1.56149	Secreted
CXCL16	Chemokine (C-X-C motif) ligand 16	2.78E-10	4.77	8.55E-08	2.57246	7.74E-06	−1.85426	Secreted
FN1	Fibronectin 1	0.623819	−1.08296	0.000859	−2.04503	0.002001	−1.88836	Secreted
NGF	Nerve growth factor (β polypeptide)	0.000775	2.67217	0.15406	1.38771	0.010828	−1.9256	Secreted
IL1B	Interleukin 1, beta	0.044493	2.36038	0.692287	1.16788	0.09088	−2.02109	Cyto/secreted
CXCL2	Chemokine (C-X-C motif) ligand 2	2.35E-08	8.4622	2.37E-05	3.03106	4.92E-05	−2.79183	Secreted
NPPB	Natriuretic peptide B	1.74E-06	8.02694	0.003829	2.37175	0.000287	−3.38439	Secreted
CXCL1	Chemokine (C-X-C motif) ligand 1	2.13E-08	18.0992	2.63E-05	4.36975	3.74E-05	−4.14194	Secreted

[a]Transcription factors.

total of 30 proteins and peptides that can be potentially secreted by epithelial cells; some were inflammatory cytokines (IL-1β, CXCL1, and CXCL2) with downregulation and others were antimicrobial peptides\proteins that were upregualted by flagellin pretreatment (S100A8, A9, LCN2, DEFB1, and Chi3l1).

Infection-induced S100A8/A9 expression is augmented by flagellin pretreatment

Having ascertained flagellin preconditioning–mediated differential expression of genes by genome-wide cDNA array, we next used PCR and immunohistochemistry to confirm the expression pattern of the two most highly induced genes: S100A8 (calgranulin A) and S100A9 (calgranulin B) in PA01-infected B6 mouse corneas. Both Real time- (**Figure 2a**) and reverse transcriptase-PCR (**Figure 2b**) revealed similar expression pattern to that detected by cDNA array for both genes; infection moderately increased their expression which was greatly enhanced by flagellin pretreatment. At the protein levels revealed by western blotting (**Figure 2c**), there were no detectable S100A8 and A9 in normal homoestatic CECs, whereas a faint band of S100A9 was seen in PA10-infected corneas. Flagellin pretreatment resulted in the expression of the pair (**Figure 2c**).

To assess the expression of these two genes at tissue levels, immunohistochemistry was performed. Although there was little staining for both S100A8 and A9 in normal controls as well as PA01-infected corneas at 6 hpi, the whole epithelial layer was positively stained with both S100A8 and A9 with strong staining at apical layer in flagellin-pretreated corneas. Confocal imaging confirmed apical expression of S100A8 and more apparent S100A9 (panels **g** and **h**, **Figure 3**). S100A8 was also found throughout the epithelial layer. There were also positive cells in the stroma, presumably the infiltrated polymorphonuclear neutrophils (PMNs) in which 45% of soluble proteins are calprotectin.[43] The expression patterns of MMP13 and MMP10 were also confirmed (data not shown), while the expression pattern of IL-1β was similar to what we previously reported.[17,44]

S100A8 and A9 neutralization decreases bacterial clearance in B6 mouse cornea.

Having shown that flagellin augments the expression of S100A8 and A9 in the cornea in response to infection, we then tested the function of S100A8 and A9 using neutralizing antibodies.[45] At 6 hpi, there was no sign of inflammation visible by slit lamp examination in all the corneas (data not shown). However, bacterial burden determination revealed a great reduction of bacterial load in mouse corneas (**Figure 4a**). S100A8 and A9 depletion increased bacterial burden 2.4- and 1.9-fold in the control and 13- and 5.6-fold in flagellin-pretreated corneas, respectively. The expression of macrophage-inflammatory protein 2 (MIP-2) had a similar pattern to bacterial load (**Figure 4b**) but myeloperoxidase activity was undetectable at this time point.

At 24 hpi, the cornea pretreated with PBS was partially opaque, whereas flagellin-pretreated corneas were clean and showed no sign of infection or inflammation (**Figure 5**). Opacity was greatly increased in the corneas injected with S100A8- or A9-neutralizing antibodies when compared with immunoglobulin G (IgG)-treated corneas without (**c** and **e** vs. **a**) or without (**d** and **f** vs. **b**) pretreatment. Compared with

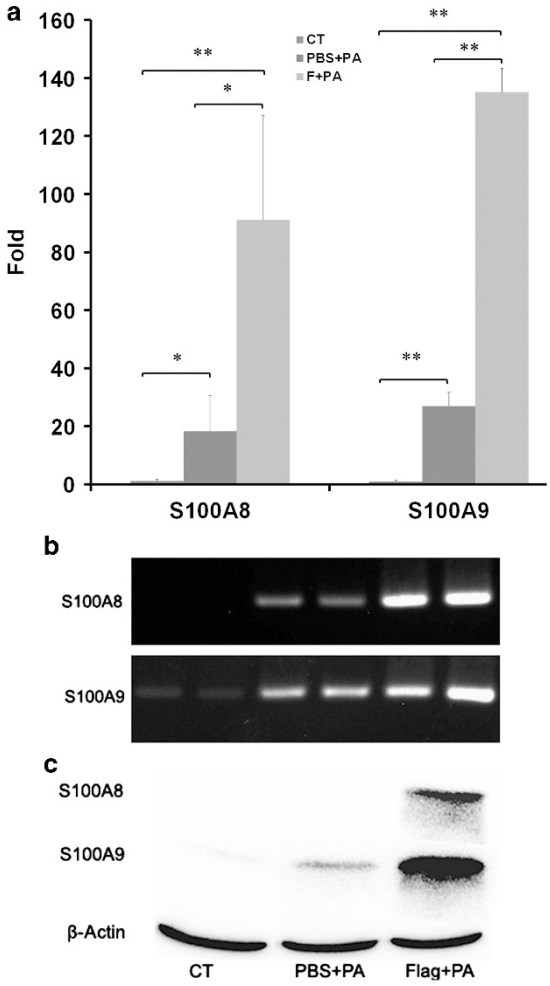

Figure 2 Infection-induced expression of S100A8 and A9 is augmented by flagellin pretreatment. B6 mice were treated as described in **Figure 1**. At 6 hpi (hours post infection), the scraped corneal epithelial cells from the control (CT), PA01-infected phosphate-buffered saline (PBS) + PA (*Pseudomonas aeruginosa*), or flagellin-pretreated and PA01-infected (Flag + PA) were subjected to (**a**) real-time PCR, (**b**) reverse transcriptase-PCR or (**c**) western blot analyses for S100A8 and A9 expression levels.

S100A9 (**e** and **f**), S100A8 neutralization resulted in more severe keratitis (**c** and **d**), and this was more apparent for flagellin-pretreated corneas (**f** vs. **d**). The different effects of S100A8 and A9 neutralizations were also observed in corneal bacterial burden, PMN infiltration, and pro-inflammatory cytokine expression. As shown in **Figure 6a**, 5.3×10^5 CFU of *P. aeruginosa* were detected in the control antibody-injected corneas while depletion of S100A8 or A9 resulted in increase of bacterial loads ~3.5-fold in the PBS-pretreated corneas. In flagellin-pretreated corneas, no recoverable bacteria were detected in control antibody-injected corneas, depletion of S100A8 and A9 resulted in 2.1×10^6 and 6.9×10^5 CFU, respectively. Similar patterns of MIP-2 expression and PMN infiltration detected by myeloperoxidase assay were also detected: in the control, PBS-pretreated corneas, S100A8 and A9 neutralization exhibited similar levels of exacerbated inflammation (elevated MIP-2 and PMN infiltration), while in flagellin-pretreated corneas, S100A8 neutralization resulted in greatly elevated inflammation comparable with that of without flagellin pretreatment and S100A9 neutralization, which, on the other hand, elevated inflammation to a level similar to PBS-pretreated corneas without neutralizing antibodies (**Figure 6b**).

DISCUSSION

In this study, we used genome-wide cDNA microarrays to identify genes expressed in CECs in response to infection, with focus on the genes differentially expressed in response to flagellin preconditioning. Our results revealed that flagellin pretreatment dramatically altered the epithelial response to infection. Contrary to the concept of tolerance or hyperresponsiveness, flagellin pretreatment augmented more than suppressed the expression of infection-induced genes at a 3:1 ratio, indicating more positive regulatory mechanisms for flagellin preconditioning–mediated gene expression in CECs. Using the data presented in the **Table 2**, we constructed a defense network elicited by flagellin pretreatment in response to infection (**Figure 7**). Although the augmented genes identified, such as CXCL10, a multifunctional chemokine with antimicrobial activity,[46] might be used as therapeutic reagents, the suppressed genes, such as MMP13, might be targeted for reducing deleterious inflammation and tissue damage in keratitis cornea.

The cDNA array analyses revealed greatly altered expression of genes in CECs in response to *P. aeruginosa* infection and illustrated the flagellin-induced alteration in gene expression at a much larger scale than that of a functional approach. In response to *P. aeruginosa*, 682 genes had more than twofold changes. The highest levels of increased genes are MMPs, AMPs, and pro-inflammatory cytokines, whereas the most downregulated gene is sestrin 1, which has a critical role in antioxidant defense in tissues, such as the retina.[47] Clearly, while innate defense mechanisms are activated in response to infection, the changes in some host genes, such as highly induced MMP13 and suppressed sestrin 1 may contribute to infection- and inflammation-associated tissue damages. In flagellin-pretreated and PA01-infected corneas, 946 genes exhibited more than twofold changes, with 907 increased and 39 decreased. The genes with the highest upregulation are S100A8 and A9, which can form the heterodimer calprotectin, a potent AMP.[41] Krt16 and Sprr2 are structural proteins and are expressed at similar levels in PA01-infected cells with or without flagellin pretreatment. Surprisingly, five genes, ifi204, IFITM3, Rsad2, ifit3, and ifi27, are IFN-stimulated genes with antiviral activity. Ifi204 and Ifitm3 may also be involved in innate defense against other microbes by regulating monocyte differentiation to macrophages and dendritic cells[48,49] and by limiting host cell proliferation to prevent spreading of pathogens,[50,51] respectively.

The most interesting comparison is between infected CECs with or without flagellin pretreatment. There are a total of 209

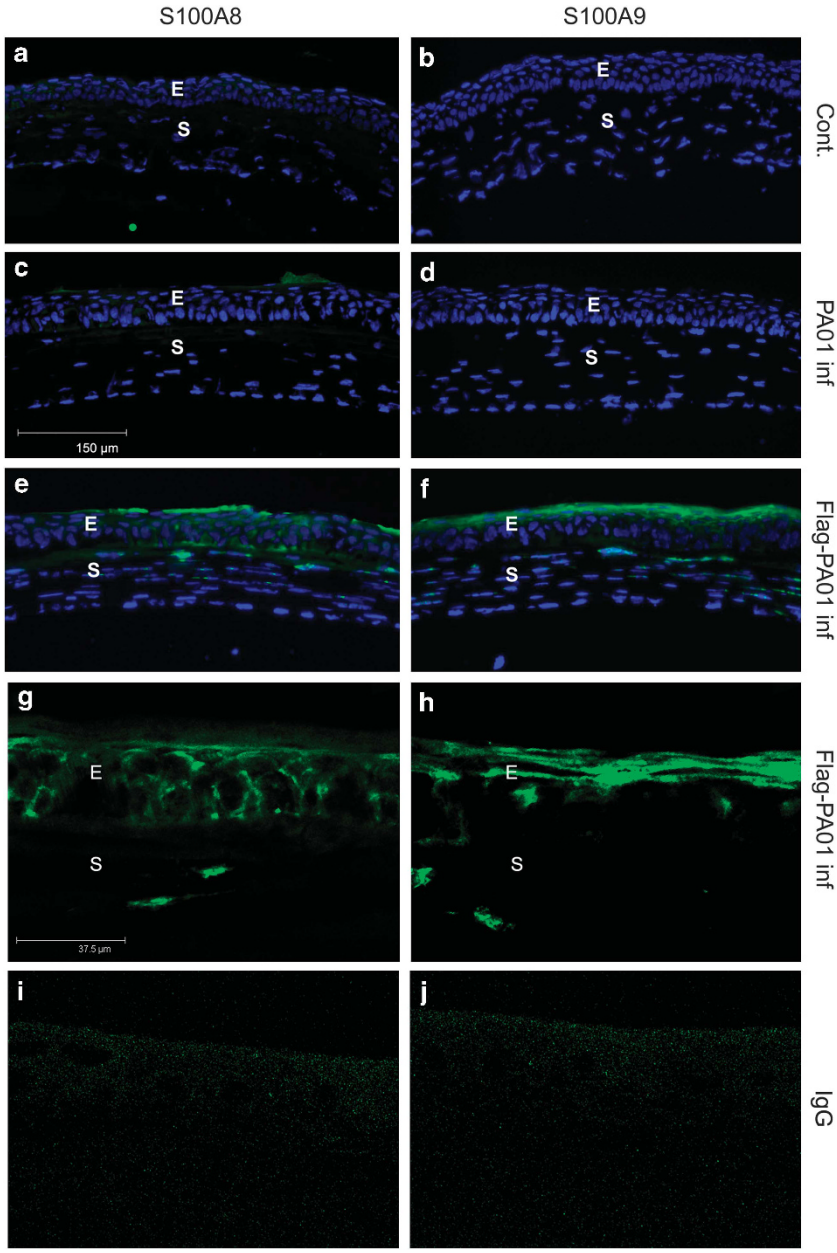

Figure 3 Immunohistochemistry of S100A8 and A9 distribution in PA01-infected and flagellin-pretreated B6 corneas. B6 mice were treated as described in **Figure 1**. At 6 hpi (hours post infection), corneas were OCT (optimal cutting temperature) snap frozen, followed by sectioning and immunostaining with antibodies against S100A8 (**a**, **c**, **e**) and S100A9 (**b**, **d**, **f**). DAPI (4,6-diamidino-2-phenylindole dihydrochloride) was used to stain nuclei. The images of S100A8 or A9 and DAPI were merged. The staining of PA01-infected and flagellin-pretreated B6 corneas with S100A8 (**g**) and S100A9 (**h**), or omitted first antibody as negative control, were also examined by confocal microscope. The figure is representative of three corneas per condition from two independent experiments. E, epithelium; IgG, immunoglobulin G; S, stroma.

genes with altered expression levels; 157 up- and 52 down-regulated. The top10 upregulated genes are mostly, with the exception of Apol9a and 9b, professional immune molecules involved in the IFN-α induction pathway with antimicrobial and/or anti-inflammatory activities. For example, Lgals3bp has been shown to activate naive and primed neutrophils, while Gbp3 I solicits defense proteins and protects the host from infection.[52] The endogenous antioxidant gene sestrin 1 was also on the list of upregulated genes (2.7 fold increase), consistent with increased protection in the cornea. On the other hand, the top 10 downregulated genes are either inflammatory molecules (IL-24, CXCL1, EGR1, SOCS3, CXCL12), proteinases/proteinase inhibitors (MMP13, MMP10, Serpina3g), or genes with unknown functions (Nppb and Prl2c3). As the altered expression of these genes results in profound innate mucosal surface protection against pathogens, many of the genes may also be involved in flagellin uniquely induced protection against other harmful environmental challenges.[31–34]

The genes were subjected to gene ontology analysis of biological processes. Prominently among different processes

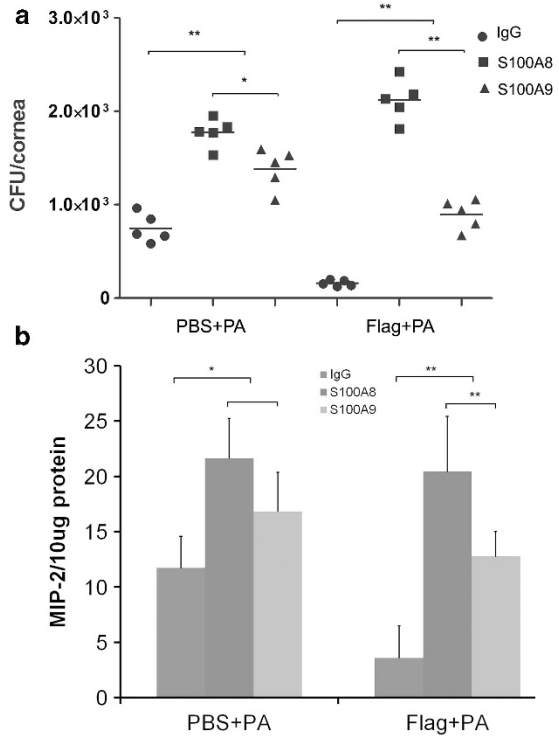

Figure 4 S100A8 and -A9 neutralization decreases bacterial clearance in B6 mouse cornea at 6 h post infection (hpi). B6 mice were pretreated with flagellin (500 ng per eye) or 5 μl phosphate-buffered saline (PBS) at −24 h and then subconjunctivally injected with 100 ng rabbit immunoglobulin G (IgG; control) or anti-S100A8- or -A9-neutralizing antibodies at −16 h. The corneas were then infected with 10^4 colony-forming units (CFU) ATCC 19660 (0 h). At 6 hpi, by which time no opacity or sign of infection was observed, the corneas were processed for (**a**) bacterial load and enzyme-linked immunosorbent assay analysis for (**b**) macrophage-inflammatory protein 2 (MIP-2). The figure is a representative of two independent experiments. $^*P \leq 0.05$, $^{**}P \leq 0.01$, $n = 5$.

are the defense response (*P*-value 1.37e-7, 83/910) and its regulation (*P*-value 2.18e-5, 34/310) that include 114 genes, some of which are overlapping in these two groups. **Table 2** listed the genes of expression levels, cellular locations, and known or suggested functions we constructed a diagram of corneal defense system activated by flagellin pretreatment (**Figure 7**). In nuclei, the pro-inflammatory transcription factor, the NF-κB family, are downregulated by flagellin pretreatment. On the other hand, four IRFs are upregulated in infected corneas, whereas IRF7 and 9 are further augmented by flagellin pretreatment. The augmented expression of these IFN-stimulated transferrins indicates that many increased genes are IFN-induced and suggests that flagellin is able to induce IFN expression and signaling. Indeed, two IFN-δ receptors, IFNGR1 and R2, are upregulated in infected CECs (**Table 2**) and, consequentially, the expression of many IFN-induced genes such as ISG15 and IFIs are also are augmented. To date, it is not clear whether IFNs are produced directly by CECs after TLR5 activation or whether IFNs are produced by residential dendritic cells and/or other innate immune cells.

Many IFN-inducible, flagellin-augmented genes are either in cytoplasm (ISG15 and OAS2) or at the cell membrane (three IFITMs). These genes are known to be dramatically induced upon viral or bacterial infection and have antiviral and innate immune activities.[50,51,53,54] The other antimicrobial proteins, LTF and S100A14, and cytoprotective PRDX5, HSP90AB1, and HSPD1 are also found in cytosol along with several ubiquitination and proteasome proteins (**Table 2**). Three TLR-related proteins can also be found in **Table 2**: MyD88, SOCS3, and SOCS6. Although MyD88 and SOCS6 remain elevated, SOCS3 expression is significantly suppressed by flagellin pretreatment. The suppressed expression of SOCS3, a suppressor of cytokine signaling,[55] is inconsistent with greatly reduced inflammation in flagellin-pretreated corneas. Interestingly, overexpression of SOCS3 has been shown to be harmful to keratinocytes by exacerbating wound inflammation.[56] Hence, its suppression by flagellin may have beneficial effects on CECs. Downregulation of intercellular adhesion molecule, an important pro-inflammatory factor, is also of importance in reducing inflammation and tissue damage caused by bacterial infection.

Among 113 defense response genes, 28 encode proteins that can be secreted by CECs. The flagellin pretreatment augmented the expression of 14 genes, most of which possess antimicrobial and innate defense activities, including S100A8, A9, Chi3l1, LCN2, CXCL10, IFIT3, IFI35, PGKYRP4, PGLYRP1, C3, and CFB (components of complement system). Synergetic effects of these factors can form a biological barrier to prevent and/or kill invading pathogens.

The altered expression of several representative genes, including S100A8, A9 (**Figure 2**), CXCL10, MMP13, -10, and Chi3l1, was confirmed by real-time or reverse transcriptase-PCR, by western blotting, and/or by immunohistochemistry. Although cDNA array revealed higher flagellin-mediated induction of S100A8 than A9, **Figure 2**, particularly western blotting appeared to suggest more pronounced upregulation of S100A9. If indeed there was more S100A9, there should have less S100A8 dimmers, which are shown to be stronger neutrophil chemoattractant.[57] Reduced S100A8 is consistent with reduced PMN infiltration observed in flagellin-pretreated corneas in response to *P. aeruginosa* infection.[17]

As S100A8 and A9 are the two most highly induced genes by flagellin pretreatment, we explored functional relevance of these two genes. S100A8 and A9 exist as noncovalently bound homodimers but also as heterodimers (S100A8/A9) that inhibit bacterial adhesion to mucosal epithelium and bacterial growth through zinc chelation.[41,43,58–60] We observed that functional blocking of both peptides significantly decreases corneal bacterial clearance at 6 and 24 hpi in the control and flagellin-pretreated corneas, providing direct evidence for bactericidal activity of these calcium-binding proteins. Interestingly, functions of S100A8 and A9 are not equal as neutralizing S100A8 appears to result in more severe keratitis than S100A9. This is more apparent in flagellin-pretreated corneas in which neutralizing S100A8 totally lost flagellin-induced protection, whereas S100A9 only partially, suggesting additional roles of S100A8. It is important to mention that while inactivation of the S100A8 gene is embryonically lethal,[61] the mice with depleted S100A9 are viable, albeit in these mice

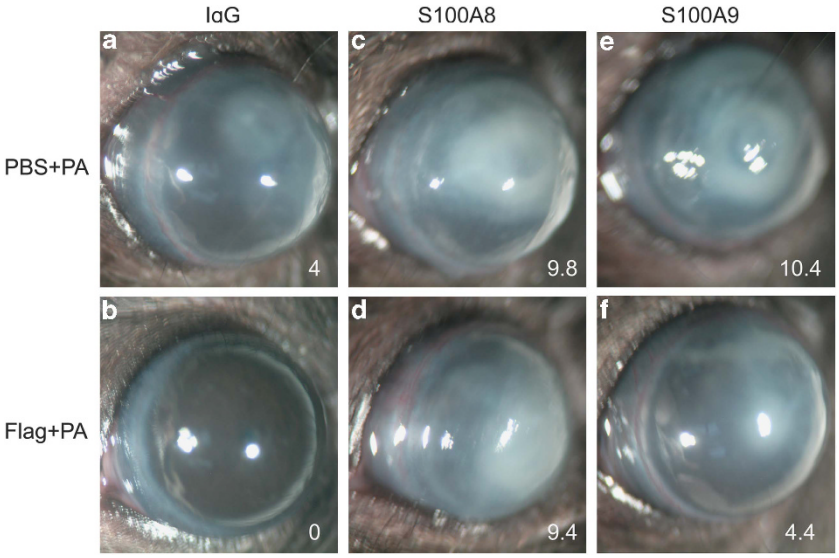

Figure 5 S100A8/9-neutralized mouse corneas are more susceptible than the wild type to *P. aeruginosa* (PA) at 1-day post infection. B6 mice were treated as described in **Figure 4** except that the mice were killed at 24 hpi (hours post infection). The corneas were photographed and clinically scored with 0 (no infection) to 12 (perforated) system.[18] The number on the low right cornea of each panel is the average clinical score of five corneas. Three independent experiments were performed, and a representative cornea was presented for each experimental condition. IgG, immunoglobulin G; PBS, phosphate-buffered saline.

S100A8 expression is not detectable,[62] suggesting non-redundant function of a member of the S100 gene family. Interestingly, while S100A8/A9 are inducible genes in epithelial cells, they are constitutively expressed in neutrophils where they comprise 45% of total cytoplasmic protein.[63,64] The abundant expression of both S100A8 and A9 in infiltrated cells of flagellin-pretreated corneas was confirmed by immunohistochemistry (**Figure 3**). Calprotectin are known to be released from neutrophils upon stimulation to form extracellular traps, which kill extracellular pathogens while minimizing damage to the host cells.[64] Hence, neutralizing S100A8 and A9 are likely to affect both epithelial-expressed and neutrophil-released S100A8/A9. Hence, our study identifies calprotectin as an important protective mediator in the innate immune response to bacterial keratitis caused by *P. aeruginosa.*

In summary, genome-wide cDNA array showed dramatic changes in the expression of many genes and revealed flagellin-elicited changes in gene expression pattern on a large scale, which would not be possible to envision by conventional approaches. The data allow us to construct an innate defense network, activation of which would result in tissue resistance to infection (**Figure 7**). Among these altered genes, the epithelially expressed S100A8 and A9 are shown to have a key role in corneal defense against the opportunistic but devastating ocular pathogen, *P. aeruginosa.* The network we constructed is of value for developing therapeutic strategies to control infection and to reduce tissue damage caused by infection-associated host inflammation.

MATERIALS AND METHODS

Bacterial strains and flagellin purification. A cytotoxic strain of *P. aeruginosa* (ATCC 19660), which provides a reproducible inflammatory response in the B6 mouse cornea,[44,65] was used to test the protective effects of flagellin and S100A8/A9. However, as cytotoxicity of strain 19660 often causes epithelial damages, we choose strain PAO1, a wound isolate and the most widely used *P. aeruginosa* laboratory strain with completely sequenced genome[66] for cDNA array study. Flagellin was prepared from PA01 by ammonium sulfate precipitation as described earlier.[22]

Mice. Wild-type C57BL6 (B6) mice (age, 8 weeks; female; weight, 20–24 g) were purchased from the Jackson Laboratory (Bar Harbor, ME). Animals were treated in compliance with the ARVO Statement for the Use of Animals in Ophthalmic and Vision Research. The Institutional Animal Care and Use Committee of Wayne State University approved all animal procedures.

Flagellin pretreatment and infection procedure. Mice were anesthetized with ketamine/xylazine and placed beneath a stereoscopic microscope at a magnification of $\times 40$ for needle scratching (three 1-mm incisions using a sterile 25-gauge needle). The injured corneas of wild type ($n = 6$ for cDNA array, $n = 5$/group for other experiments) were pretreated with 500 ng purified flagellin in 5 µl of PBS or PBS (the control) by topical application. For infection, the treated corneas were re-scratched and inoculated by topical application of bacterial suspension (5 µl) containing 1×10^4 CFU of strain ATCC 19660 or 1×10^5 CFU of strain PA01. Eyes were examined daily to monitor the disease progression.

RNA extraction and real-time PCR. For RNA isolation, epithelial cells were scraped off six corneas, two pooled into one tube as one sample, of naive (the Control), infected, and flagellin-pretreated/infected mice and frozen in liquid nitrogen immediately. RNA was extracted from the collected epithelial cells using RNeasy Mini Kit (Qiagen, Valencia, CA), according to the manufacturer's instructions. cDNA was generated with an oligo(dT) primer (Invitrogen, Life Technologies, Grand Island, NY) followed by analysis using real-time PCR with the Power SYBR Green PCR Master Mix (AB Applied Biosystems, University Park, IL) based on the expression of β-actin. The following primer pairs were used: 5′-GACGGCCAGGTCATCACTATTG-3,′ 5′-AGGAAGGCTGGAAAAGAGCC-3′ for β -Actin, 5′-TGC GAT GGT

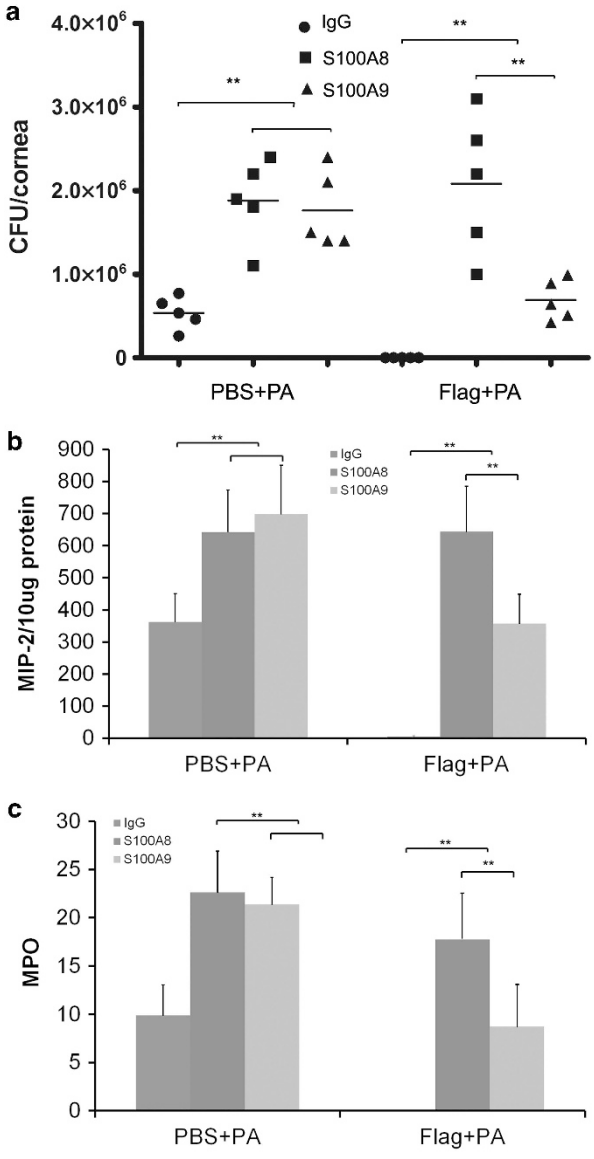

Figure 6 Topical flagellin is ineffective in protecting the cornea from *P. aeruginosa* S100A8/9-neutralized mice cornea. The corneas presented in **Figure 5** were subjected to (**a**) bacteria counting, (**b**) macrophage-inflammatory protein 2 (MIP-2) expression determined by enzyme-linked immunosorbent assay, and (**c**) myeloperoxidase (MPO) determination (units per cornea). $^{*}P \leq 0.05$ and $^{**}P \leq 0.01$, $n = 5$. CFU, colony-forming units; IgG, immunoglobulin G; PBS, phosphate-buffered saline.

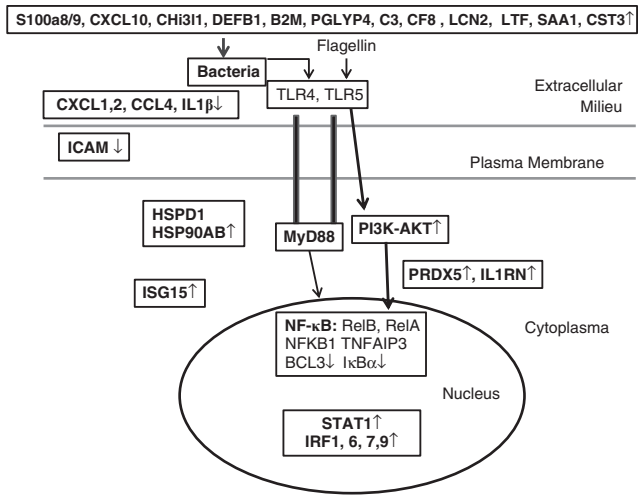

Figure 7 The diagram shows flagellin-induced defense response to microbial infection in the ocular surface. An innate defense network, activation of which will result in tissue resistance to infection, was constructed using the data presented in **Table 2**. A myriad of genes are expressed in response to infection and flagellin pretreatment may suppress (↓), have no effects, or augment (↑) the expression of these genes. Transcription factors distributed in the nuclei regulates (long arrowheads) the expression of cytoprotective (blue) and defense (green), inflammatory (red) genes that form an effective defense network against microbial infection starting from extracellular space, to plasma membrane and to cytosol without excessive inflammation as many pro-inflammatory factors are suppressed by flagellin pretreatment.

GAT AAA AGT GG-3′, 5′-GGC CAG AAG CTC TGC TAC TC-3′ for S100A8 and 5′-CAC AGT TGG CAA CCT TTA TG-3′, 5′-CAG CTG ATT GTC CTG GTT TG-3′ for S100A9.

Gene array and functional analysis. Epithelial cells of normal control, PA01-infected, and flagellin-pretreated and PA01-infected B6 mouse corneas were scrapped off with dulled thin blade, scooped epithelial cells were frozen immediately in liquid nitrogen, removed from the blade with a forceps into an 1.5-ml Eppendorf tube placed on dry ice with two corneas pooled in one tube. Total RNA from pooled epithelial cells was isolated using RNeasy (Qiagen). RNA quality was verified using the Bioanalyzer (Agilent Technologies, Santa Clara, CA, USA). cDNAs were synthesized and hybridized to an Illumina mouse WG-6v2.0 expression bead chip containing 45,200 50-mer transcripts. Data were collected at Applied Genomics Technology Center, Wayne State Univerisity School of Medicine and evaluated by Genomic Core Lab of National Institute of Diabetes and Digestive and Kidney Diseases, Bethesda, MD, USA. The analysis of variance analysis for the RMA-normalized data sets was done by the commercial microarray data analysis software Partek Genomic Suite http://www.partek.com/partekgs/. Signaling pathway and functional network analyses were performed using Genomatrix Pathways System software.

Immunohistochemistry of mouse corneas. Mouse eyes were enucleated and embedded in Tissue-Tek optimal cutting temperature compound and frozen in liquid nitrogen. Six-micrometer thick sections were cut and mounted to polylysine-coated glass slides. After a 10-min fixation in 4% paraformaldehyde, slides were blocked with 10 mM sodium phosphate buffer containing 2% bovine serum albumin for 1 h at room temperature. Sections were then incubated with mouse primary antibody (S100A8 1:200 and S100A9 1:100, R&D Systems, Minneapolis, MN). This was followed by a secondary antibody, FITC anti-rat or anti-goat IgG (Jackson ImmunoResearch Laboratories; 1:100), and slides were mounted with Vectashield mounting medium containing 4, 6-diamidino-2-phenylindole dihydrochloride (DAPI) mounting media and examined under a Carl Zeiss fluorescence microscope Axioplan 2 equipped with an ApoTome digital camera or using confocal microscopy (TCSSP2; Leica). Controls were similarly treated, but the primary antibody was replaced with rat or rabbit IgG.

S100A8/9 neutralization and infection. Purified flagellin (500 ng in 5 µl of PBS) or PBS (control) was topically applied on the cornea before *P. aeruginosa* challenge. Sixteen hours before *P. aeruginosa* inoculation, B6 mice were subconjunctivally injected 5 µl PBS containing 0.5 mg ml^{-1} of rabbit anti-mouse S100A8/9 (kindly provided by Dr Philippe Tessier). The control mice received the same dose of rabbit IgG. The eyes were inoculated with 1×10^4 CFU of strain ATCC 19660.

Bacterial burden determination, cytokine ELISA, and myeloperoxidase measurement. Bacterial load, ELISA determination of MIP-2, and myeloperoxidase measurements were performed as described, and the same mouse cornea was used in all the three assays.[18]

Statistical analyses. Data were presented as means ± s.d. Statistical differences among three or more groups were identified using one-way analysis of variance. Differences were considered statistically significant at $P<0.05$.

SUPPLEMENTARY MATERIAL is linked to the online version of the paper at http://www.nature.com/mi

ACKNOWLEDGEMENTS
This study was supported by grants NIH/NEI R01-EY010869, R01-EY017960, P30-EY004068, R01-HL097564, Midwest Eye Bank, Research to Prevent Blindness.

DISCLOSURE
The authors declared no conflict of interest.

REFERENCES

1. Kawai, T. & Akira, S. Toll-like receptors and their crosstalk with other innate receptors in infection and immunity. *Immunity* **34**, 637–650 (2011).
2. Nish, S. & Medzhitov, R. Host defense pathways: role of redundancy and compensation in infectious disease phenotypes. *Immunity* **34**, 629–636 (2011).
3. Weindl, G., Wagener, J. & Schaller, M. Epithelial cells and innate antifungal defense. *J. Dent. Res.* **89**, 666–675 (2010).
4. Ueta, M. & Kinoshita, S. Innate immunity of the ocular surface. *Brain Res. Bull.* **81**, 219–228 (2010).
5. Muller, C.A., Autenrieth, I.B. & Peschel, A. Innate defenses of the intestinal epithelial barrier. *Cell. Mol. Life Sci.* **62**, 1297–1307 (2005).
6. Parker, D. & Prince, A. Innate immunity in the respiratory epithelium. *Am. J. Respir. Cell Mol. Biol.* **45**, 189–201 (2011).
7. Ben Mkaddem, S., Chassin, C. & Vandewalle, A. Contribution of renal tubule epithelial cells in the innate immune response during renal bacterial infections and ischemia-reperfusion injury. *Chang Gung Med J* **33**, 225–240 (2010).
8. Marques, R. & Boneca, I.G. Expression and functional importance of innate immune receptors by intestinal epithelial cells. *Cell. Mol. Life Sci.* **68**, 3661–3673 (2011).
9. Swamy, M., Jamora, C., Havran, W. & Hayday, A. Epithelial decision makers: in search of the 'epimmunome'. *Nat. Immunol.* **11**, 656–665 (2010).
10. Sun, Y., Hise, A.G., Kalsow, C.M. & Pearlman, E. Staphylococcus aureus-induced corneal inflammation is dependent on Toll-like receptor 2 and myeloid differentiation factor 88. *Infect. Immun.* **74**, 5325–5332 (2006).
11. Botturi, K. *et al.* Preventing asthma exacerbations: what are the targets?. *Pharmacol. Ther.* **131**, 114–129 (2011).
12. Wang, Y., Bai, C., Li, K., Adler, K.B. & Wang, X. Role of airway epithelial cells in development of asthma and allergic rhinitis. *Respir. Med.* **102**, 949–955 (2008).
13. Lang, T. & Mansell, A. The negative regulation of Toll-like receptor and associated pathways. *Immunol. Cell Biol.* **85**, 425–434 (2007).
14. West, M.A. & Heagy, W. Endotoxin tolerance: A review. *Crit. Care Med.* **30**, S64–S73 (2002).
15. Vartanian, K. & Stenzel-Poore, M. Toll-like receptor tolerance as a mechanism for neuroprotection. *Transl. Stroke Res.* **1**, 252–260 (2010).
16. Biswas, S.K. & Lopez-Collazo, E. Endotoxin tolerance: new mechanisms, molecules and clinical significance. *Trends Immunol.* **30**, 475–487 (2009).
17. Kumar, A., Gao, N., Standiford, T.J., Gallo, R.L. & Yu, F.S. Topical flagellin protects the injured corneas from *Pseudomonas aeruginosa* infection. *Microbes Infect.* **12**, 978–989 (2010).
18. Gao, N., Kumar, A., Guo, H., Wu, X., Wheater, M. & Yu, F.S. Topical flagellin-mediated innate defense against Candida albicans keratitis. *Invest. Ophthalmol. Vis. Sci.* **52**, 3074–3082 (2011).
19. Cursiefen, C. Immune privilege and angiogenic privilege of the cornea. *Chem. Immunol. Allergy* **92**, 50–57 (2007).
20. Hamrah, P. & Dana, M.R. Corneal antigen-presenting cells. *Chem. Immunol. Allergy* **92**, 58–70 (2007).
21. Kumar, A. & Yu, F.S. Toll-like receptors and corneal innate immunity. *Curr. Mol. Med.* **6**, 327–337 (2006).
22. Zhang, J., Xu, K., Ambati, B. & Yu, F.S. Toll-like receptor 5-mediated corneal epithelial inflammatory responses to *Pseudomonas aeruginosa* flagellin. *Invest. Ophthalmol. Vis. Sci.* **44**, 4247–4254 (2003).
23. Fleiszig, S.M. & Evans, D.J. Contact lens infections: can they ever be eradicated?. *Eye Contact Lens* **29**, S67–S71 (2003). discussion S83-64, S192-194.
24. Alarcon, I., Kwan, L., Yu, C., Evans, D.J. & Fleiszig, S.M. Role of the corneal epithelial basement membrane in ocular defense against *Pseudomonas aeruginosa*. *Infect. Immun.* **77**, 3264–3271 (2009).
25. Fleiszig, S.M. & Evans, D.J. Pathogenesis of contact lens-associated microbial keratitis. *Optom. Vis. Sci.* **87**, 225–232 (2010).
26. Szczotka-Flynn, L.B., Pearlman, E. & Ghannoum, M. Microbial contamination of contact lenses, lens care solutions, and their accessories: a literature review. *Eye Contact Lens* **36**, 116–129 (2010).
27. Ibrahim, Y.W., Boase, D.L. & Cree, I.A. Epidemiological characteristics, predisposing factors and microbiological profiles of infectious corneal ulcers: the Portsmouth corneal ulcer study. *Br. J. Ophthalmol.* **93**, 1319–1324 (2009).
28. Hazlett, L.D. Bacterial infections of the cornea (*Pseudomonas aeruginosa*). *Chem. Immunol. Allergy* **92**, 185–194 (2007).
29. Kumar, A., Singh, C.N., Glybina, I.V., Mahmoud, T.H. & Yu, F.S. Toll-like receptor 2 ligand-induced protection against bacterial endophthalmitis. *J. Infect. Dis.* **201**, 255–263 (2010).
30. Yu, F.S. *et al.* Flagellin stimulates protective lung mucosal immunity: role of cathelicidin-related antimicrobial peptide. *J. Immunol.* **185**, 1142–1149 (2010).
31. Burdelya, L.G. *et al.* An agonist of toll-like receptor 5 has radioprotective activity in mouse and primate models. *Science* **320**, 226–230 (2008).
32. Vijay-Kumar, M. *et al.* Flagellin treatment protects against chemicals, bacteria, viruses, and radiation. *J. Immunol.* **180**, 8280–8285 (2008).
33. Kinnebrew, M.A., Ubeda, C., Zenewicz, L.A., Smith, N., Flavell, R.A. & Pamer, E.G. Bacterial flagellin stimulates Toll-like receptor 5-dependent defense against vancomycin-resistant Enterococcus infection. *J. Infect. Dis.* **201**, 534–543 (2010).
34. Jarchum, I., Liu, M., Lipuma, L. & Pamer, E.G. Toll-like receptor-5 stimulation protects mice from acute *Clostridium difficile* colitis. *Infect. Immun.* **79**, 1498–1503 (2011).
35. Miao, E.A. *et al.* Cytoplasmic flagellin activates caspase-1 and secretion of interleukin 1beta via Ipaf. *Nat. Immunol.* **7**, 569–575 (2006).
36. Miao, E.A., Andersen-Nissen, E., Warren, S.E. & Aderem, A. TLR5 and Ipaf: dual sensors of bacterial flagellin in the innate immune system. *Semin. Immunopathol.* **29**, 275–288 (2007).
37. Uematsu, S. & Akira, S. Immune responses of TLR5(+) lamina propria dendritic cells in enterobacterial infection. *J. Gastroenterol.* **44**, 803–811 (2009).
38. Carvalho, F.A., Aitken, J.D., Gewirtz, A.T. & Vijay-Kumar, M. TLR5 activation induces secretory interleukin-1 receptor antagonist (sIL-1Ra) and reduces inflammasome-associated tissue damage. *Mucosal Immunol.* **4**, 102–111 (2010).
39. Hsu, K. *et al.* Anti-Infective protective properties of S100 calgranulins. *Anti-inflammatory Anti-allergy Agents Med. Chem.* **8**, 290–305 (2009).
40. Brandtzaeg, P., Gabrielsen, T.O., Dale, I., Muller, F., Steinbakk, M. & Fagerhol, M.K. The leucocyte protein L1 (calprotectin): a putative nonspecific defence factor at epithelial surfaces. *Adv. Exp. Med. Biol.* **371A**, 201–206 (1995).
41. Liu, J.Z. *et al.* Zinc sequestration by the neutrophil protein calprotectin enhances Salmonella growth in the inflamed gut. *Cell Host Microbe* **11**, 227–239 (2012).
42. Dela Cruz, C.S. *et al.* Chitinase 3-like-1 Promotes Streptococcus pneumoniae Killing and Augments Host Tolerance to Lung Antibacterial Responses. *Cell Host Microbe* **12**, 34–46 (2012).

43. Lusitani, D., Malawista, S.E. & Montgomery, R.R. Calprotectin, an abundant cytosolic protein from human polymorphonuclear leukocytes, inhibits the growth of Borrelia burgdorferi. *Infect. Immun.* **71**, 4711–4716 (2003).
44. Kumar, A., Hazlett, L.D. & Yu, F.S. Flagellin suppresses the inflammatory response and enhances bacterial clearance in a murine model of *Pseudomonas aeruginosa* keratitis. *Infect. Immun.* **76**, 89–96 (2008).
45. Raquil, M.A., Anceriz, N., Rouleau, P. & Tessier, P.A. Blockade of antimicrobial proteins S100A8 and S100A9 inhibits phagocyte migration to the alveoli in streptococcal pneumonia. *J. Immunol.* **180**, 3366–3374 (2008).
46. Crawford, M.A. *et al.* Antimicrobial effects of interferon-inducible CXC chemokines against Bacillus anthracis spores and bacilli. *Infect. Immun.* **77**, 1664–1678 (2009).
47. Doonan, F., Wallace, D.M., O'Driscoll, C. & Cotter, T.G. Rosiglitazone acts as a neuroprotectant in retinal cells via up-regulation of sestrin-1 and SOD-2. *J. Neurochem.* **109**, 631–643 (2009).
48. Bourette, R.P. & Mouchiroud, G. The biological role of interferon-inducible P204 protein in the development of the mononuclear phagocyte system. *Front. Biosci.* **13**, 879–886 (2008).
49. Rouabhia, M., Ross, G., Page, N. & Chakir, J. Interleukin-18 and gamma interferon production by oral epithelial cells in response to exposure to Candida albicans or lipopolysaccharide stimulation. *Infect. Immun.* **70**, 7073–7080 (2002).
50. Siegrist, F., Ebeling, M. & Certa, U. The small interferon-induced transmembrane genes and proteins. *J. Interferon Cytokine Res.* **31**, 183–197 (2011).
51. Hofman, V.J. *et al.* Gene expression profiling in human gastric mucosa infected with Helicobacter pylori. *Mod. Pathol.* **20**, 974–989 (2007).
52. Kim, B.H., Shenoy, A.R., Kumar, P., Das, R., Tiwari, S. & MacMicking, J.D. A family of IFN-gamma-inducible 65-kD GTPases protects against bacterial infection. *Science* **332**, 717–721 (2011).
53. Kim, K.I., Malakhova, O.A., Hoebe, K., Yan, M., Beutler, B. & Zhang, D.E. Enhanced antibacterial potential in UBP43-deficient mice against Salmonella typhimurium infection by up-regulating type I IFN signaling. *J. Immunol.* **175**, 847–854 (2005).
54. Liu, C.S., Sun, Y., Zhang, M. & Sun, L. Identification and analysis of a *Sciaenops ocellatus* ISG15 homologue that is involved in host immune defense against bacterial infection. *Fish Shellfish Immunol.* **29**, 167–174 (2010).
55. Caruso, R. *et al.* Inhibition of monocyte-derived inflammatory cytokines by IL-25 occurs via p38 Map kinase-dependent induction of Socs-3. *Blood* **113**, 3512–3519 (2009).
56. Linke, A., Goren, I., Bosl, M.R., Pfeilschifter, J. & Frank, S. Epithelial overexpression of SOCS-3 in transgenic mice exacerbates wound inflammation in the presence of elevated TGF-beta1. *J. Invest. Dermatol.* **130**, 866–875 (2010).
57. Yano, J., Lilly, E., Barousse, M. & Fidel, Jr P.L. Epithelial cell-derived S100 calcium-binding proteins as key mediators in the hallmark acute neutrophil response during Candida vaginitis. *Infect. Immun.* **78**, 5126–5137 (2010).
58. Nisapakultorn, K., Ross, K.F. & Herzberg, M.C. Calprotectin expression in vitro by oral epithelial cells confers resistance to infection by Porphyromonas gingivalis. *Infect. Immun.* **69**, 4242–4247 (2001).
59. Nisapakultorn, K., Ross, K.F. & Herzberg, M.C. Calprotectin expression inhibits bacterial binding to mucosal epithelial cells. *Infect. Immun.* **69**, 3692–3696 (2001).
60. Murthy, A.R., Lehrer, R.I., Harwig, S.S. & Miyasaki, K.T. In vitro candidastatic properties of the human neutrophil calprotectin complex. *J. Immunol.* **151**, 6291–6301 (1993).
61. Passey, R.J. *et al.* A null mutation in the inflammation-associated S100 protein S100A8 causes early resorption of the mouse embryo. *J. Immunol.* **163**, 2209–2216 (1999).
62. Manitz, M.P. *et al.* Loss of S100A9 (MRP14) results in reduced interleukin-8-induced CD11b surface expression, a polarized microfilament system, and diminished responsiveness to chemoattractants in vitro. *Mol. Cell Biol.* **23**, 1034–1043 (2003).
63. Edgeworth, J., Gorman, M., Bennett, R., Freemont, P. & Hogg, N. Identification of p8,14 as a highly abundant heterodimeric calcium binding protein complex of myeloid cells. *J. Biol. Chem.* **266**, 7706–7713 (1991).
64. Achouiti, A. *et al.* Myeloid-related protein-14 contributes to protective immunity in gram-negative pneumonia derived sepsis. *Plos Pathog.* **8**, e10029872012).
65. Hazlett, L.D., McClellan, S., Kwon, B. & Barrett, R. Increased severity of *Pseudomonas aeruginosa* corneal infection in strains of mice designated as Th1 versus Th2 responsive. *Invest. Ophthalmol. Vis. Sci.* **41**, 805–810 (2000).
66. Stover, C.K. *et al.* Complete genome sequence of *Pseudomonas aeruginosa* PA01, an opportunistic pathogen. *Nature* **406**, 959–964 (2000).